Progress In Electromagnetics Research Letters, Vol. 112, 87–95, 2023

Metamaterial-Inspired Notebook Antenna with 2.4/5/6 GHz Wi-Fi 7 Operation

Saou-Wen Su* **and Muhammad I. Magray**

Abstract—A metamaterial-inspired antenna is proposed that utilizes an artificial mu-negative (MNG) transmission line (TL) to incorporate the zeroth-order resonance (ZOR) into Wi-Fi 7 operation in the 2.4/5/6 GHz wireless local area network (WLAN) bands. The antenna comprises a meta-structured loop with periodically loaded series interdigital capacitors and a parasitic shorted strip, all formed on the same substrate layer in a coplanar structure. The 2.4 and 6 GHz bands are produced by the parasitic strip and the close-form loop strip, respectively, which are of typical right-handed antennas. The 5 GHz band caused by the ZOR mode, where the permeability is zero, can be adjusted by the series capacitance in the unit cell. The total antenna size is 5.4 mm × 19.6 mm only. In this work, the design applied to notebook computers for the upcoming Wi-Fi 7 operation is also demonstrated. Both numerical and experimental results validate our proof-of-concept design.

1. INTRODUCTION

The demand for faster data rates has increased significantly in the past two decades. To meet this demand, wireless devices now require multiple antennas to support more spatial streams. The Federal Communications Commission (FCC) has approved the addition of an unlicensed 6 GHz band (5925–7125 MHz) to work alongside Wi-Fi 6 (IEEE 802.11ax) networks [1]. This expanded bandwidth of 1200 MHz enables faster wireless speeds and lower latency services. It is very important to note that Wi-Fi 6E not only includes the 5925–7125 MHz range but also covers the 2.4 GHz (2400–2484 MHz) and 5 GHz (5150–5825 MHz) wireless local area network (WLAN) bands. In the notebook industry, it has become standard for antennas to operate in the 2.4/5/6 GHz bands, and accordingly various low-profile 2.4/5/6 GHz notebook antennas have been developed for slim-bezel displays [2–13]. Meanwhile, Wi-Fi 7 (IEEE 802.11be) [14], the successor to Wi-Fi 6/6E, is currently being developed and tested by the IEEE task group and major chip manufacturers. Wi-Fi 7 is expected to provide speeds 3.6 times faster than Wi-Fi 6, with up to 320 MHz per access point and support multi-link operation, allowing data aggregation across different frequency bands. Note that both Wi-Fi 7 and Wi-Fi 6E cover the same 2.4, 5, 6 GHz WLAN bands.

Metamaterials have been demonstrated to have a profound impact on antenna applications [15–23]. The composite right/left-handed (CRLH) transmission line (TL) has been widely studied in antenna designs [15, 16, 22, 23], which show unique resonant characteristics of exhibiting an infinite-wavelength wave at the zeroth-order resonance (ZOR) frequency [15, 16]. However, compared with CRLH-TL antennas, the epsilon-negative (ENG)- or mu-negative (MNG)-TL antennas are simpler in structure that comprises either one artificially added shunt inductance (L_{LH}) or series capacitance (C_{LH}). In addition, the ENG- and MNG-TL antennas can also support the ZOR mode with the same infinite-wavelength properties [17–21]. Nevertheless, most of the metamaterial antennas [15–23] focus on meta-structures,

Received 12 June 2023, Accepted 6 September 2023, Scheduled 21 September 2023

* Corresponding author: Saou-Wen Su (Saou-Wen_Su@asus.com).
The authors are with the Antenna Design Department, Advanced EM & Wireless Communication R&D Center, ASUSTek Computer Inc., Taipei 11259, Taiwan.

mode characteristics, equivalent circuit models, and are proposed with stand-alone architecture or in a bulky structure. Very seldom are the metamaterial antenna designs seen applied to the terminal devices, for example, mobile phones and notebook computers. Terminal devices have limited space for antenna engineers. The antennas for terminal devices must be designed with the device system ground considered, unlike metamaterial-TL antennas designed in stand-alone architecture [15–23] without being integrated with the device ground. The conventional metamaterial antenna topology is not practical for terminal devices with limited space, especially using the CRLH-TL structure [24, 25]. Given that factor, the authors were motivated to design a metamaterial-inspired antenna that is very practical for industrial notebook computers and for Wi-Fi 7 operation.

The proposed antenna comprises an MNG-TL strip, a parasitic shorted strip, and a soldering ground, all on the same substrate layer. For this meta-structured design, a close-form loop strip is selected. The MNG-TL strip has periodically loaded series capacitors. Three unit cells are structured to achieve the ZOR mode for operating in the 5 GHz WLAN band. In addition, the 2.4 and 6 GHz WLAN bands are excited, respectively, by the parasitic strip and the close-form loop of conventional RH-TL antennas. To the best of the authors' knowledge, an MNG-TL-based notebook antenna has not been reported anywhere in the open literature. In addition, we structure unit cells to achieve the ZOR mode as extra resonance in addition to the RH loop resonant mode for obtaining a wideband in the 5/6 GHz WLAN bands. The metamaterial TL is not designed in stand-alone architecture [15–23], but rather incorporated into the conventional RH antenna, thus not increasing the overall antenna size. Also, compared with the existing MNG-TL structures in [19–21], which show rather large periodical structures, the proposed structure and design topology are more practical for terminal device applications.

This article is structured as follows. In Section 2, the antenna design structure is elaborated upon, and the contribution to antenna resonant modes is discussed. Section 3 verifies the proof-of-concept design prototype through numerical and experimental results. Lastly, Section 4 provides a concise conclusion. Throughout the article, the proposed design and its results are discussed in detail.

2. MNG-TL-BASED NOTEBOOK ANTENNA DESIGN

Figure 1(a) illustrates the geometry of the proposed metamaterial-incorporated antenna. The design is formed on a 0.8-mm-thick, single-layered FR4 substrate with relative permittivity 4.4 and loss tangent 0.024, size 5.4 mm × 19.6 mm and located above a 14-inch display frame for possible notebook applications. This metal frame has a size of 1 mm × 182 mm × 315 mm and is also utilized as a large system ground plane in notebook designs. Note that a 15 mm keep-out-zone from the side edge ($+x$ direction) to the antenna is required as it is reserved for mechanical-assembly design purpose.

The design primarily comprises an MNG-TL strip, a parasitic shorted strip, and a soldering ground, all on the same layer in a coplanar structure. The MNG TL requires a short-ended boundary condition [19] and has periodically loaded series capacitors. For the design of the MNG-TL-based antenna, a close-form loop strip is selected. The artificial capacitances are realized by using interdigital capacitors. The dimensions of the interdigital capacitors are detailed in Fig. 1(b). The finger length of 0.8 mm and total width of 1.4 mm with four fingers are designed. In this work, three unit cells are structured to achieve the ZOR mode in the 5 GHz band. In addition, the 2.4 and 6 GHz bands are excited, respectively, by the parasitic strip (with a quarter-wavelength monopole mode) and the close-form loop (with a half-wavelength loop mode) of the conventional RH-TL antennas. That is, a tri-band Wi-Fi 7 operation can be obtained in the 2.4/5/6 GHz WLAN bands.

Note that the MNG materials have a rejection band in the lower frequencies and an RH-TL propagation band in the higher frequencies. Accordingly, the ZOR was designed in the 5 GHz band, while the 6 GHz band was excited by the RH mode of the antenna. In addition, the L-shaped parasitic strip is placed within the vacant space formed by the meta-structured loop strip, which prevents an increase in the overall size of the design. Parameter simulations were performed using the electromagnetic solver, Ansys HFSS [26]. A photograph of the proposed antenna is shown in Fig. 1(c). A semi-rigid coaxial cable of length about 70 mm was used in experiments for feeding the fabricated prototype over the diminutive feed gap of 0.5 mm.

To better understand the operating mechanism of the design, a simple loop and the design without the parasitic strip are first analyzed in Fig. 2(a). It is seen that the simple loop produces one resonance

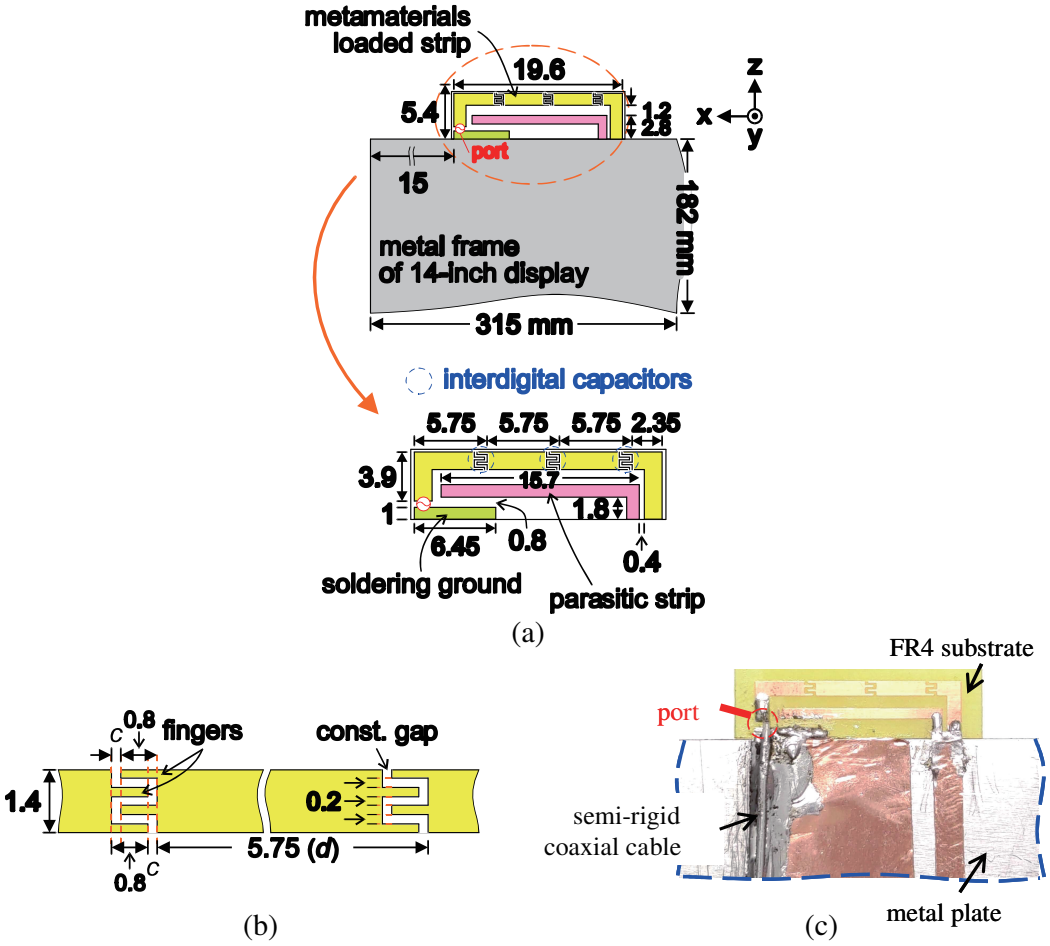

Figure 1. (a) Geometry of the metamaterial-incorporated coplanar antenna. (b) Detailed dimensions of the interdigital capacitor. (c) Photography of a fabricated prototype.

at 5400 MHz, whereas the loop strip loaded with three series capacitors as an MNG TL can achieve two separate modes at 4920 and 6780 MHz in the upper bands. In this case, the loop mode shifts from 5400 MHz to 6780 MHz, and the MNG TL produces an additional mode at ZOR frequency around 4.9 GHz. Compared with the proposed antenna, the design without the parasitic strip (the MNG-TL strip only) have no resonance in the lower band for 2.4 GHz operation. This suggests that this shorted strip mainly contributes to the 2.4 GHz band.

$$\omega_{series} = \frac{1}{\sqrt{L_{RH}C_{LH}}} \tag{1}$$

In this study, the location of the ZOR mode can be slightly fine-tuned by the diminutive gap c. As seen in Fig. 2(b), with a decrease in the gap c, the ZOR frequency decreases. This is because the series capacitance increases with a smaller gap and the ZOR frequency is inversely proportional to the square root of the product of series inductance (L_{RH}) and capacitance (C_{LH}) [15]. In the case, the ZOR mode can be evaluated by using (1). In general, to obtain a lower ZOR frequency, the numbers of fingers or the unit-cell length (series inductance) need to be increased. Although the 0.1 mm gap shows a little wider impedance bandwidth over the 5 and 6 GHz bands, this diminutive value will cause higher tolerance in PCB manufacturing, which is not preferred. Note that to keep the analyses simpler, the vertical parts of the gap remain the same at 0.2 mm; only the horizontal parts vary here. The results also show that the resonant mode for the 2.4 GHz band is about the same, while the 6 GHz band loop resonance is slightly affected owing to the nearby ZOR frequency. In addition, comparing the cases of three unit cells in Fig. 2(a) and the two unit cells only in Fig. 2(c), the ZOR frequencies (4.9 vs.

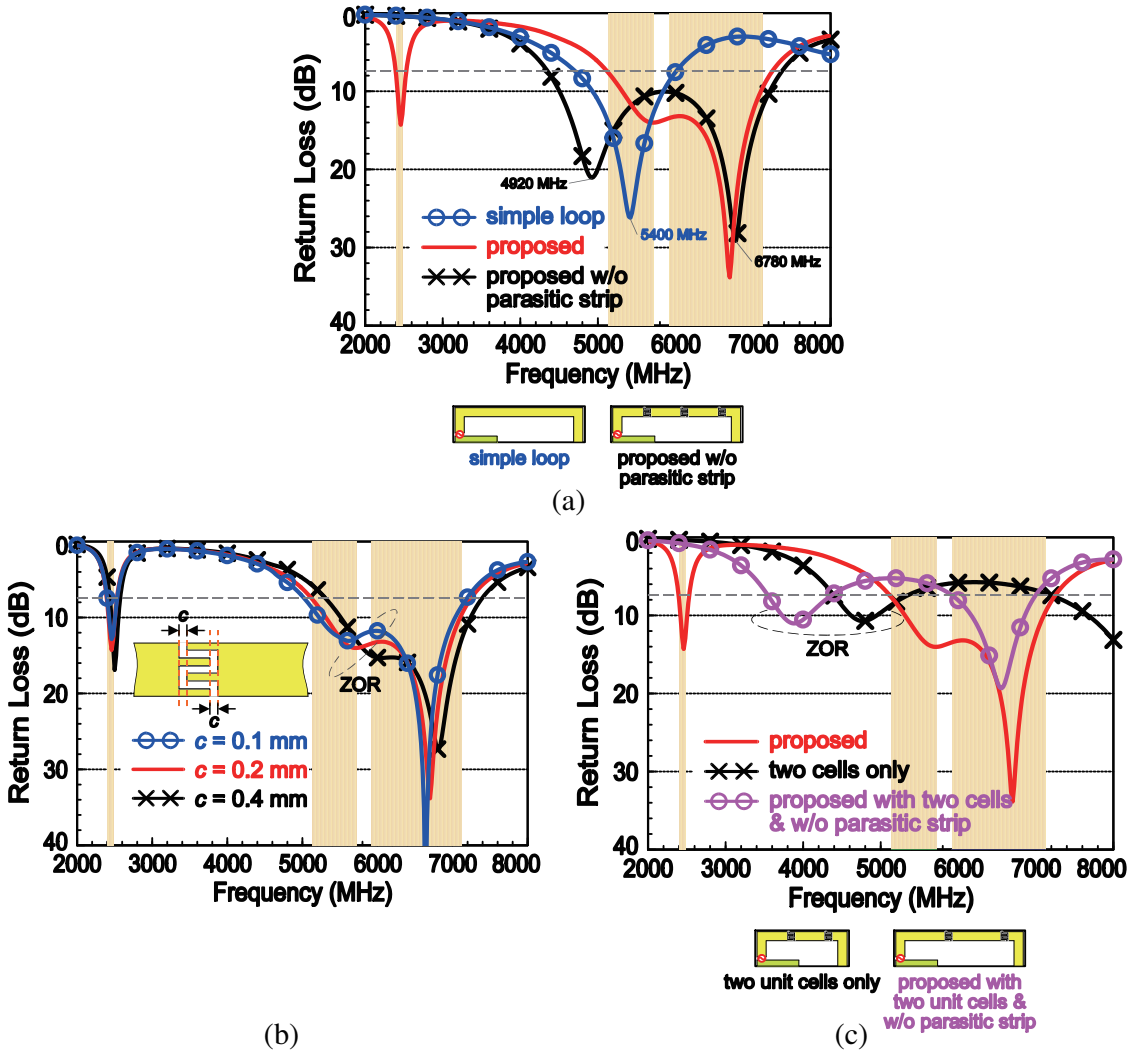

Figure 2. Simulated return losses for (a) the simple loop and the proposed w/o the parasitic strip ($d = 5.75$ mm), (b) various gap c of the interdigital capacitor, and (c) the two cells only ($d = 5.75$ mm) and the proposed with two cells ($d = 8.625$ mm); both w/o parasitic strip.

4.8 GHz) are very similar, which indicates the infinite-wavelength wave occurred at around 4.8–4.9 GHz.

For the meta-structured simple loop, two possible cases of the MNG-TL loop strip with two unit cells are also investigated and compared. The two structures can be seen in the insets of Fig. 2(c). The first case is of the two unit cells only with $d = 5.75$ mm and a total lateral length of 13.85 mm. The second case is of the proposed simple loop of the same lateral length of 19.6 mm as the design in Fig. 1(a) but with $d = 8.625$ mm. It can been seen that the ZOR frequencies for these two cases are not the same owing to different unit-cell lengths (d), which change the series inductances and thereby affect the ZOR frequencies. The longer the length d is, the lower the ZOR frequency becomes. The results also indicate that the 6 GHz band resonance (with RH-TL attribute) is determined by the resonant length of the close-form loop strip.

The unit cell and the equivalent circuit thereof are depicted in Fig. 3(a). The unit cell is simulated, and the constitutive parameters and the dispersion diagram are analyzed in Figs. 3(b) and 3(c), respectively. From the parameter extraction of the unit cell, it is seen that the permittivity (ε) is a positive value for the entire antenna operating bands and the permeability (μ) shows a transition from negative to positive values around 4.8 GHz, which validates that the design has the MNG-metamaterial properties.

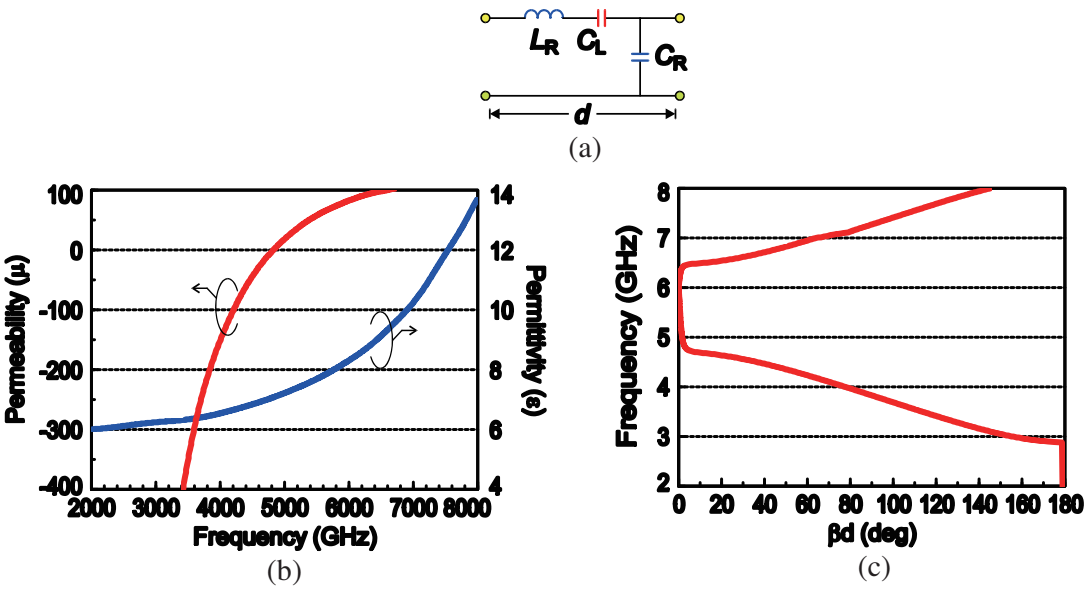

Figure 3. (a) Circuit model of the unit cell. (b) Constitutive parameters of the unit cell. (b) Dispersion diagram of the unit cell.

3. RESULTS AND DISCUSSIONS

Figure 4 gives the simulated and measured return losses for the proposed antenna and the fabricated prototype. The 2.4, 5, and 6 GHz bands are marked by the colored bars. The experimental result agrees fairly well with the numerical data. Some discrepancies found are probably attributed to the PCB manufacturing tolerance for the interdigital capacitors and the routing of the feeding cable in the measurement. The input matching over the frequency bands of interest for 2.4/5/6 GHz Wi-Fi 7 operation all surpasses the 7.3 dB return loss (about VSWR of 2.5).

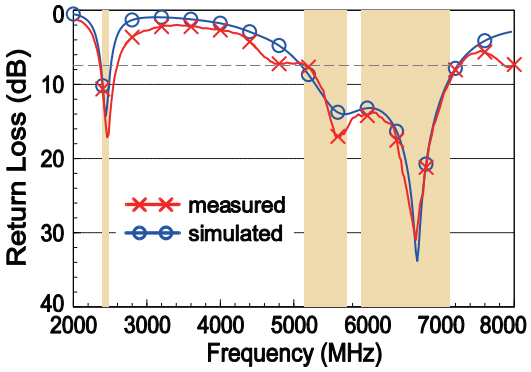

Figure 4. Simulated and measured return losses.

The current distributions of the design excited at 2480, 5740, and 6720 MHz are presented in Fig. 5(a). The current intensity in the color bar is kept the same for these frequencies of different mode excitation. First, for the 2480 MHz mode, it is clearly seen that large currents are distributed on the parasitic strip, and it is identified as a quarter-wavelength monopole mode. As for the two resonant modes at 5740 and 6720 MHz in the upper bands, more currents are found on the meta-structured loop strip. It is important to see that in-phase currents at 5740 MHz are observed (see black arrows along the loop strip), which supports an infinite-wavelength wave at the ZOR mode. Lastly, a current null

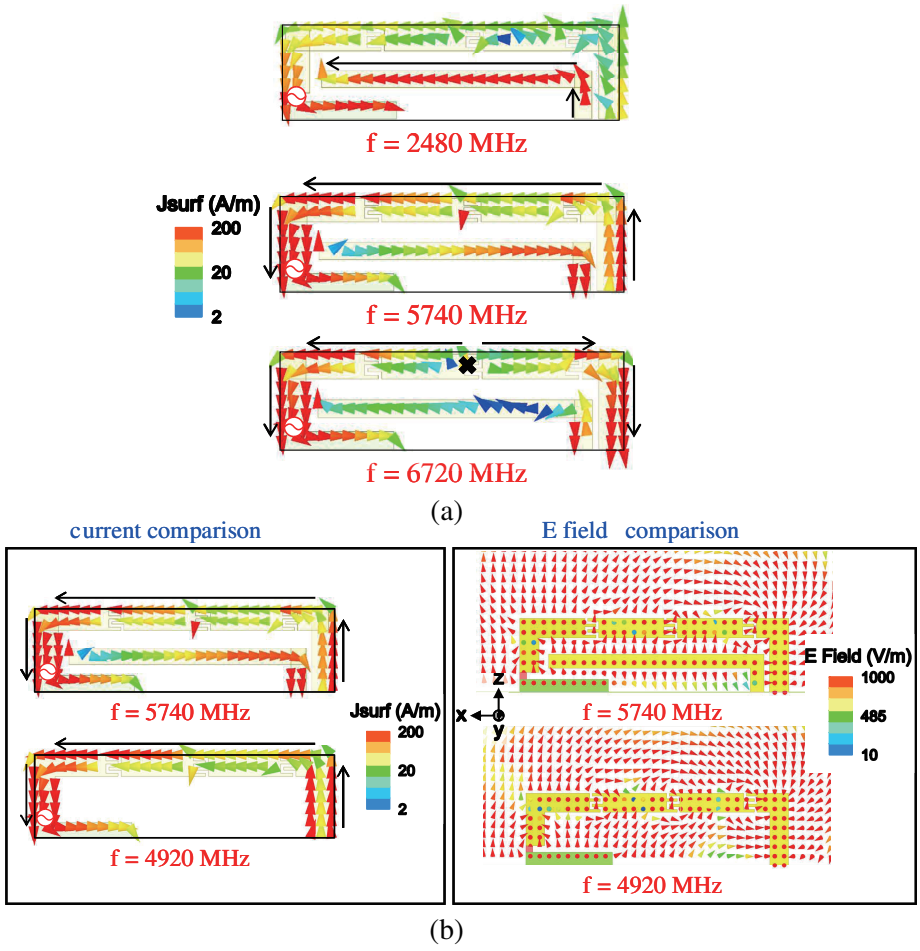

Figure 5. (a) Surface current distributions at 2480, 5740, and 6720 MHz for the proposed design. (b) Comparison on the current and electric field distributions at the ZOR frequency for the proposed design and the proposed w/o the parasitic strip.

at 6720 MHz observed by opposite vector currents around the middle of the loop strip is seen, which represents a half-wavelength loop mode. In addition, compared with the design without the parasitic strip [see inset in Fig. 2(a)], the same in-phase currents at the ZOR mode can also be observed, as shown in Fig. 5(b). It is also seen in Fig. 5(b) that the electric fields of these ZOR modes at different frequencies have the same distributions surrounding the antenna above the display. Owing to the in-phase currents, the electric fields on the strips of both cases are in the same direction with vector fields entering the $-y$ direction. Note that the electric fields were simulated in the x-z plane of the antenna coordinate defined in Fig. 1(a). These phenomena show again that the contributions of the monopole, the MNG-TL, and the loop modes are related to the three excited resonant modes of the proposed notebook antenna design.

Figures 6(a), 6(b), 6(c) plot the simulated and measured 2-D radiation patterns at 2480, 5740, and 6720 MHz. In our anechoic chamber, we utilized the MVG SG 24 systems equipped with multi-probe technology [27] to acquire the far-field patterns. Notably, the E-total fields are presented instead of separate E_θ and E_ϕ fields, as both polarizations coexist in multipath environments. Additionally, based on our empirical studies on notebook measurement, the E-total gain patterns correlated significantly with the throughput performance results. In the 2.4 GHz band, larger field intensity in the $+z$ direction with symmetrical patterns in the y-z plane is first observed. As for the 5/6 GHz bands, the symmetrical patterns in the y-z plane are also found. However, owing to different operating mechanisms, the patterns at 5740 and 6720 MHz are not exactly the same. In general, more radiation energy is found toward the

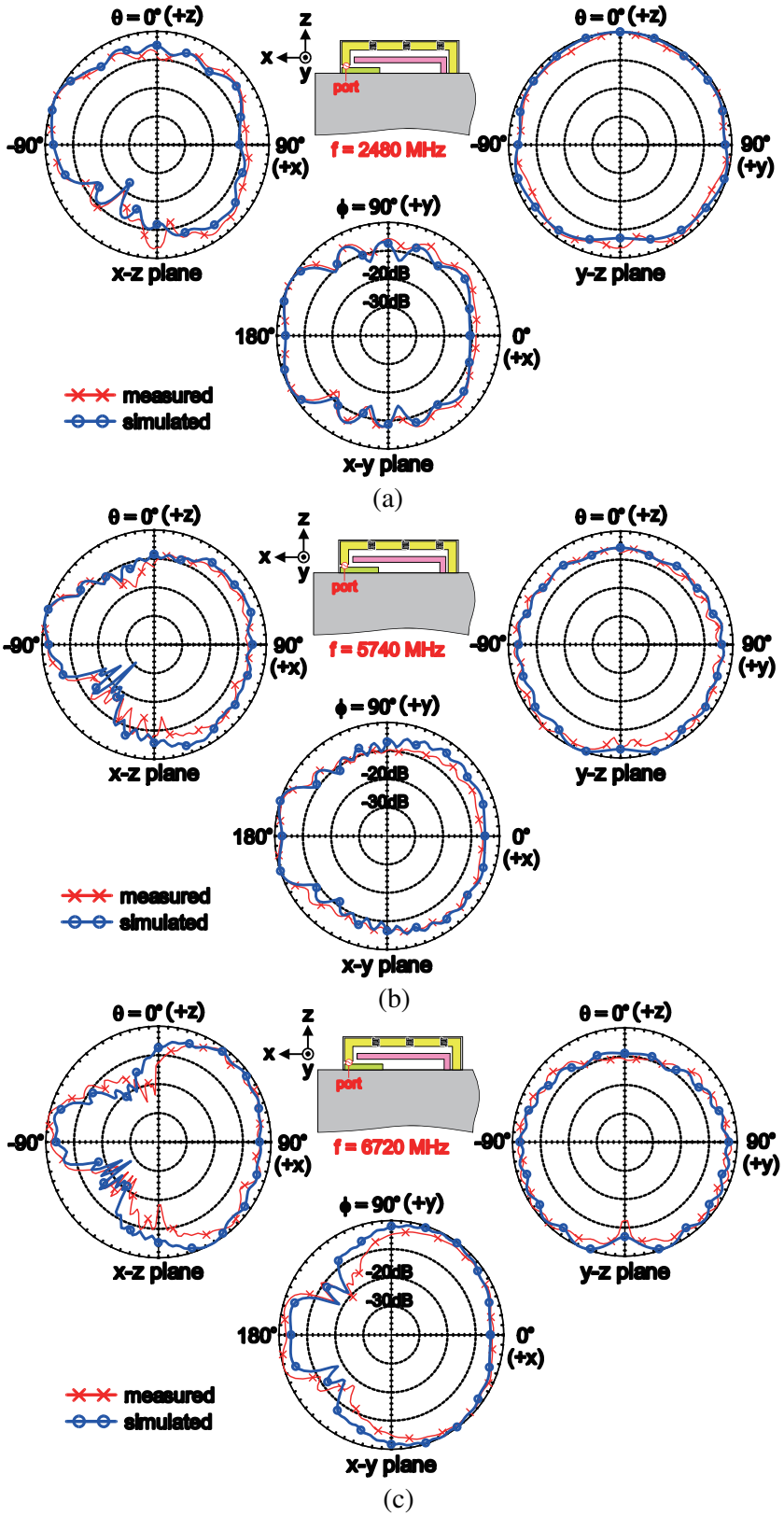

Figure 6. Simulated and measured 2-D radiation patterns (E-total) at (a) 2480, (b) 5740, and (c) 6720 MHz.

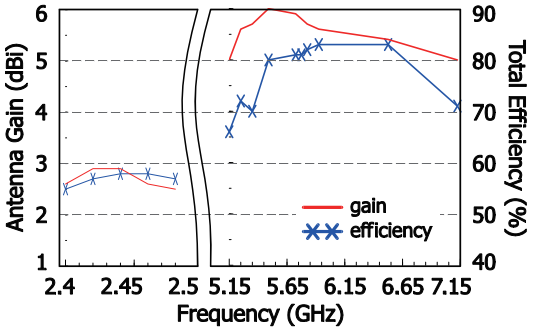

Figure 7. Measured peak antenna gain and total efficiency.

$+x$ direction.

Figure 7 shows the measured peak antenna gain (E-total) and total efficiency (antenna efficiency) [28]. In the experiments, the cable loss and antenna mismatching in the return losses are all included. The obtained peak gain in the 2.4 GHz band is about 2.5–2.9 dBi with total efficiency exceeding 55%. For the 5/6 GHz bands, the peak gain is in the range of 5.0 to 6.0 dBi with efficiency about 66 to 83%.

4. CONCLUSION

A multi-resonant printed antenna operating in the 2.4/5/6 GHz Wi-Fi 7 bands for notebook computer applications has been introduced and verified. The design utilizes an MNG-TL structure built into a loop strip to achieve the ZOR resonance for 5 GHz operation. The close-form loop strip also produces a higher RH resonant mode in the 6 GHz band. The ZOR mode of the MNG-TL structure is incorporated to widen the impedance bandwidth of the simple loop antenna for covering the entire 5 and 6 GHz bands. Together, these two modes cover the 5150–7125 MHz frequency range. In addition, the antenna produces one RH resonance in the lower 2.4 GHz band using the parasitic strip encompassed by the MNG-TL loop strip. Good radiation properties have also been observed. The proposed metamaterial-inspired antenna design is very practical and appealing for industrial notebook antennas.

REFERENCES

1. Federal Communications Commission, "FCC opens 6 GHz band to Wi-Fi and other unlicensed uses," https://www.fcc.gov/document/fcc-opens-6-ghz-band-wi-fi-and-other-unlicensed-uses-0.
2. Lee, C. T., C. C. Wan, and S. W. Su, "Multi-laptop-antenna designs for 2.4/5/6 GHz WLAN and 5G NR77/78/79 operation," *Proc. Int. Symposium on Antennas and Propagat.*, 421–422, Osaka, Japan, 2020.
3. Su, S. W., D. P. Yusuf, and F. H. Chu, "Conjoined, Wi-Fi 6E MIMO antennas for laptops," *Proc. Int. Symposium on Antennas and Propagat.*, 1–2, Taipei, Taiwan, 2021.
4. Su, S. W. and C. C. Wan, "Asymmetrical, self-isolated laptop antenna in the 2.4/5/6 GHz Wi-Fi 6E bands," *Proc. Int. Symposium on Antennas and Propagat.*, 1–2, Taipei, Taiwan, 2021.
5. Su, S. W., "Compact, small, chip-inductor-loaded Wi-Fi 6E monopole antenna," *Proc. IEEE Int. Symposium on Antennas Propagat.*, 937–938, Singapore, 2021.
6. Sim, C. Y. D., et al., "A PIFA design with WLAN and Wi-Fi 6E band for laptop computer applications," *Proc. IEEE Int. Symposium on Antennas Propagat.*, 1808–1809, Denvor, USA, 2022.
7. Su, S. W., "Miniaturized, Wi-Fi 6E notebook antenna using an in-series chip inductor," *IEEE Int. Workshop on Electromagnetics*, 168–169, Chiba, Japan, 2022.
8. Yusuf, D. P., F. H. Chu, and S. W. Su, "Ultra-wideband Wi-Fi 6E/5G NR antenna for laptop applications," *Asia-Pacific Microw. Conf.*, 548–550, Yokohama, Japan, 2022.

9. Sim, C. Y. D., J. Kulkarni, S. H. Wang, S. Y. Zheng, Z. H. Lin, and S. C. Chen, "Low-profile laptop antenna design for Wi-Fi 6E band," *IEEE Antennas Wireless Propagat. Lett.*, Vol. 22, 79–83, 2023.
10. Magray, M. I., S. W. Su, and D. P. Yusuf, "Electrically small, conformal Wi-Fi 6E antenna for compact laptop devices," *Arabian J. Sci. Eng.*, 1–7, 2023.
11. Su, S. W., P. H. Juan, and F. S. Chang, "Conjoined, two-monopole antenna pair with decoupling inductor for Wi-Fi 6E notebook applications," *Int. J. Antennas Propagat.*, Vol. 22, 1–8, 2022.
12. Su, S. W. and P. H. Juan, "Miniaturized antenna pair for 2.4/5/6 GHz Wi-Fi 6E operation," *Progress In Electromagnetics Research Letters*, Vol. 107, 39–47, 2022.
13. Juan, P. H. and S. W. Su, "EMC hybrid loop/monopole LDS antenna with three-sided ground walls for 2.4/5/6 GHz WLAN operation," *IEEE Antennas Wireless Propagat. Lett.*, Vol. 22, 1–5, 2023, early access.
14. Garcia-Rodriguez, A., D. López-Pérez, L. Galati-Giordano, and G. Geraci, "IEEE 802.11be: Wi-Fi 7 strikes back," *IEEE Comm. Mag.*, Vol. 21, 102–108, 2021.
15. Sanada, A., C. Caloz, and T. Itoh, "Novel zeroth-order resonance in composite right/left-handed transmission line resonators," *Asia-Pacific Microw. Conf.*, 1588–1591, Seoul, South Korea, 2003.
16. Caloz, C. and T. Itoh, *Electromagnetic Metamaterials: Transmission Line Theory and Microwave Applications*, Wiley, 2006.
17. Lai, A., K. M. K. H. Leong, and T. Itoh, "Infinite wavelength resonant antennas with monopolar radiation pattern based on periodic structures," *IEEE Trans. Antennas Propagat.*, Vol. 55, 868–876, 2007.
18. Park, J.-H., Y.-H. Ryu, J.-G. Lee, and J.-H. Lee, "Epsilon negative zeroth-order resonator antenna," *IEEE Trans. Antennas Propagat.*, Vol. 55, 3710–3712, 2007.
19. Park, J.-H., Y.-H. Ryu, and J.-H. Lee, "Mu-zero resonance antenna," *IEEE Trans. Antennas Propagat.*, Vol. 58, 1865–1875, 2010.
20. Wei, K., Z. Zhang, Z. Feng, and M. F. Iskander, "A MNG-TL loop antenna array with horizontally polarized omnidirectional patterns," *IEEE Trans. Antennas Propagat.*, Vol. 60, 2702–2710, 2012.
21. Wei, K., Z. Zhang, Z. Feng, and M. F. Iskander, "A wideband MNG-TL dipole antenna with stable radiation patterns," *IEEE Trans. Antennas Propagat.*, Vol. 61, 2418–2424, 2013.
22. Alibakhshikenari, M., B. S. Virdee, L. Azpilicueta, et al., "A comprehensive survey of "metamaterial transmission-line based antennas design challenges and applications"," *IEEE Access*, Vol. 8, 144778–144808, 2020.
23. Zhang, J., S. Yan, and G. A. E. Vandenbosh, "Composite right/left-handed transmission line metamaterial-inspired small antenna design: Topologies, reconfigurability, and applications," *IEEE Antennas Propagat. Mag.*, Vol. 65, 71–78, 2023.
24. Bertin, G., B. Piovano, and R. Vallauri, "Metamaterial-inspired antennas for telecommunication applications," *European Conf. Antennas Propagat. (EuCAP)*, 1–2, Prague, Czech Republic, 2012.
25. Suhas, D. and S. Bhattacharyya, "Compact dual-band CRLH metamaterial planar antenna in laptops for WLAN/WiMAX frequencies," *IEEE Microw. Antennas Propagat. Conf. (MAPCON)*, 1037–1042, Bangalore, India, 2022.
26. Ansys HFSS, Ansys Inc., http://www.ansys.com/Products/Electronics/ANSYS-FSS.
27. SG 24-S, MVG, https://www.mvg-world.com/en/products/antenna-measurement/multi-probe-systems/sg-24.
28. Balanis, C. A., *Antenna Theory: Analysis and Design*, Wiley, 2016.